Earth Science Research; Vol. 2, No. 1; 2013
ISSN 1927-0542 E-ISSN 1927-0550
Published by Canadian Center of Science and Education

Electrofacies Modelling and Lithological Classification of Coals and Mud-bearing Fine-grained Siliciclastic Rocks Based on Neural Networks

Paula Schmitt[1], Mauricio R. Veronez[1], Francisco M. W. Tognoli[1], Viviane Todt[1], Ricardo C. Lopes[2] & Carlos A. U. Silva[3]

[1] Graduate Program on Geology, Vale do Rio dos Sinos University, São Leopoldo, Brazil

[2] Geology Course, Vale do Rio dos Sinos University, São Leopoldo, Brazil

[3] Transport Engineering Department, Ceará Federal University, Fortaleza, Brazil

Correspondence: Mauricio R. Veronez, Graduate Program on Geology, Vale do Rio dos Sinos University, São Leopoldo, Brazil. Tel: 55-51-3591-1122 ext. 1731. E-mail: veronez@unisinos.br

Received: April 16, 2012 Accepted: May 2, 2012 Online Published: December 18, 2012

doi:10.5539/esr.v2n1p193 URL: http://dx.doi.org/10.5539/esr.v2n1p193

Abstract

The identification of lithofacies from well is usually an interpretative process based on geophysical logs since core and sidewall samples are not usually available. Despite being always sampled and described, cuttings are useful only as a reference for determining the rocks because a number of problems occur during the drilling and sampling activities. Well logs are *in situ* continuous records of different physical properties of the drilled rocks, which can be associated with different lithofacies by experienced log analysts. This task needs a relatively great amount of time and it is likely to be imperfect because the human analysis is subjective. Thus, any alternative method of classification with high accuracy and promptness is very welcome by the log analysts. This paper is based on Neural Networks (NNs) applied in well data from the Leão Coal Mine, southern Brazil, in order to classify organic mudrocks, coals and siliciclastic sandstones, the main rocks present in the Rio Bonito and Palermo formations, by using their well logs as database. The training and validation set of the NN contain data from eight cored and logged boreholes. The input included 409 values of depth and logs of gamma-ray, spontaneous potential, resistance and resistivity for each electrofacies. The neural network model was the feedforward multilayer perceptron (MLP) and the neural networks were trained with variations of the backpropagation algorithm: Levenberg-Marquardt and Resilient backpropagation. Although an accuracy of approximately 80% had been achieved in the general classification, discrepant accuracies in the classification of the different electrofacies are discussed in order to better understand the reasons that affected negatively the NN performance.

Keywords: well logs, artificial intelligence, supervised classification, Leão Coal Mine, Paraná Basin, Brazil

1. Introduction

The rock sampling in a well which crosses intervals that bear mineral resources of any nature (e.g.: water, oil, gas, coal, metals, etc.) is essential for understanding its genesis and the subsequent activities of research and/or exploitation. Drill-cores and sidewall samples are obtained along intervals of interest, taking into account that continuous cores and the sidewall samples are punctual. They are used for determining the type of rock as well as for quantifying a number of properties through laboratory analyses. Nevertheless, very high costs restrict these kind of samples from being obtained throughout the well. Cutting samples are continuously recuperated, but they do have limitations regarding the correct positioning and reliable representation of the rock in the drilled succession.

As a way to increase the feasibility of continuous sampling in subsurface, the measuring of several properties by means of sensors is a usual procedure, like natural radioactivity, electrical conductivity, transit time of sound waves, among others. The measuring of properties is part of the logging operations, usually carried out throughout the well. The values obtained in these operations are processed and transformed into continuous records of variations along the well, named geophysical logs, well logs or electrical logs.

Well logs have become more accurate as technology developed and presently allow initial analysis of many aquifers and oil fields to be done based only on the log interpretation. In order to fill the lack of rock samples and to avoid harming the assessment on the interval of interest, combined log analysis is a common practice. It allows estimate, for instance, the kind of rock, to recognize permeable layers, to identify intervals bearing hydrocarbons and to determine the percentage of rock porosity.

For many decades, well log analysis was done manually and visually for the identification of rocks. The identification was carried out mainly by means of cutoffs, that is, intervals with values previously determined for a given kind of rock in one or more logs (e.g., shales and sandstones using gamma ray). The use of such method required an experienced log analyst who could relate the standards obtained to the different lithological types. Although good enough, that method demands a relatively great amount of time for the analysis of one single well or interval. It is also subject to different criteria of standard recognition as well as it is limited to human capacity to simultaneously relate data that may vary in nature. On the other hand, many researchers have developed different approaches in order to automate the process in the last years. A number of techniques has been used, such as statistical (Busch et al., 1987; Flexa et al., 2004; Sancevero et al., 2008), fuzzy logic (Toumani et al., 1994; Saggaf & Nebrija, 2003a; Ilkhchi et al., 2006) and neural network (Baldwin et al., 1990; Rogers et al., 2002; Bhatt & Helle, 2002; Saggaf & Nebrija, 2000, 2003b; Maiti et al., 2007; Schmitt, 2009; Maiti & Tiwari, 2010; Raeesi et al., 2012). Specific applications of neural networks for better understand organic and fine-grained siliciclastic rocks from well logs are rare (e.g., Huang & Williamson, 1996; Yang et al., 2004; Schmitt, 2009). Thus, a selected dataset was chosen for testing the neural network accuracy in differentiating these types of rocks.

This paper aims to recognize electrofacies patterns and link them specifically to organic and fine-grained siliciclastic rocks of the Rio Bonito and Palermo formations at the Leão Coal Mine through neural network. The results were based on 28% of training data and 72% of validation data and allowed a discussion of the variable indexes of the network accuracy, since the well logs intervals of training and validation are cored and the original descriptions were used to compare with the results. Besides, the lithological features of the working site challenge the achievement of a successful quality of training and validation and also challenge the results of the lithofacies classification as a consequence. Although with a general accuracy of approximately 80% in the validation phase, a number of problems were identified and discussed in order to better understand the quality of the results.

2. Neural Networks and Electrofacies Modelling

Neural Networks (NN) are groupings of processing units, called neurons or nodes, structured and interconnected, whose functionality is similar to a neural structure of intelligent organisms. The NN have a high computational power due to its parallel and distributed structure and its capacity to learn and/or make generalizations, what makes it possible to solve complex problems in a vast range of scientific knowledge(Haykin, 1999).

In view of its non-linear structure, the NN is capable to capture the most complex characteristics from the data, which is not always possible if one uses the traditional statistical techniques or other deterministic methods. The greatest advantage of neural networks over conventional methods, such as the statistical one, is to carry out an analysis without knowledge of the intrinsic theory of the matter. Other great advantages are to analyze relations which are not fully known among the variables involved in the modelling and use a well-established technique for application in well log data.

The use of numerical-computational methods for the classification of rocks based on well logs started in the early 70's and it was boosted from the late 80's. Those first works were based on numerical (Harris & McCammon, 1971; Doveton & Cable, 1979) and statistical methods, especially the principal component analysis (Wolff & Pelissier-Combescure, 1982) and the discriminant analysis (Busch et al., 1987; Delfiner, 1987). The classification of rocks based on artificial intelligence methods applied to well logs came up in the early 90's, following the works that had been carried out on neural networks (Derek et al., 1990; Baldwin et al., 1990; Rogers et al., 1992; Benaouda et al., 1999; Zhang et al., 1999; Saggaf & Nebrija, 2000; Siripitayananon et al., 2001; Bhatt, 2002; Bhatt & Helle, 2002; Yang et al., 2004; Maiti et al., 2007; Maiti & Tiwari, 2010) and fuzzy logic (Toumani et al., 1994; Xuyan & Zhanglong, 1998; Saggaf & Nebrija, 2003a; Hsieh et al., 2005). The basic principle is to identify the log patterns associated with facies or facies associations in different well logs, named electrofacies, and structure a neural network in order to recognize such patterns in all the succession or study area.

Saggaf and Nebrija (2000) performed a supervised analysis to identify rocks previously identified from cores. The automatic method proposed by the authors was based on competitive neural network and had similar results

to those performed by experienced log analysts. Furthermore, the method provides a way to measure the degree of confidence of the analysis. Another application on electrofacies modeling estimated missing logs in wells with a incomplete suite (Saggaf & Nebrija, 2003b). The authors recognized the interdependence among different logs using as example a well with a complete log suite and applied a neural network to estimate the missing logs. The high accuracy of the results was evaluated by blind tests in which both estimated log and the real one were compared. An interesting application of neural networks was performed by Yang et al. (2004). They estimated the clay content, grain density, total organic carbon and cement using mudstone and carbonate values obtained from well logs.

3. Resilient Backpropagation and Levenberg-Marquardt Algorithms

The Resilient Backpropagation (Rprop) is an algorithm that performs batch supervised training in multilayer perceptron-like networks. This algorithm works in order to eliminate the negative influence of the partial derivative value in the weight adjustment. This influence occurs because the output value of a neuron of approximately 0 (or 1) and the expected output of 1 (or 0) imply in a derivative of approximately 0. Thus, the weight for this neuron will be minimally adjusted (Braga et al., 2007).The Rprop is capable to eliminate this problem using just the signal of the derivative, not its value. The signal indicates the direction of the weight adjustment, either increasing or decreasing the previous weight. The range of the weight adjustment is given by the "actualization value" $\Delta^t{}_{ji}$, as shown by Equation 1.

$$\Delta w_{ji}(t) = \begin{cases} -\Delta_{ji}(t), if \ \dfrac{\partial E}{\partial w_{ji}}(t) > 0 \\ +\Delta_{ji}(t), if \ \dfrac{\partial E}{\partial w_{ji}}(t) < 0 \\ 0, if \ \dfrac{\partial E}{\partial w_{ji}} = 0 \end{cases} \tag{1}$$

The Δ_{ji} is defined as an adaptation process dependent of the signal of the error derivative in relation with the weight to be adjusted, as indicated by Equation 2.

$$\Delta w_{ji}(t) = \begin{cases} \eta^+ \Delta_{ji}(t-1), if \ \dfrac{\partial E(t-1)}{\partial w_{ji}} \dfrac{\partial E(t)}{\partial w_{ji}} > 0 \\ \eta^- \Delta_{ji}(t-1), if \ \dfrac{\partial E(t-1)}{\partial w_{ji}} \dfrac{\partial E(t)}{\partial w_{ji}} < 0 \\ \Delta_{ji}(t-1), if \ \dfrac{\partial E}{\partial w_{ji}} = 0 \end{cases} \tag{2}$$

Where:

$$0 < \eta^- < 1 < \eta^+$$

According with the rule of adaption used by Rprop, when the partial derivative of the error in relation to the weight w_{ji} keeps the same sign (indicating that the last adjust decreased the error), the actualization value Δ_{ji} increases by the factor η^+ and speeds up the training convergence. When the partial derivative changes the sign (indicating that the last adjust was too much), the actualization value Δ_{ji} decreases by the factor η^- and changes the direction of adjustment.

The Levenberg-Marquardt algorithm is an approximation of the Newton's method. It improves the Gauss-Newton method by using a variable learning rate and was proposed to adjust the weights of the neural network after each cycle. This algorithm is a numerical optimization technique of high computational complexity which spends a great volume of memory, which might impede its utilization in huge networks (Haykin, 1999).

When this algorithm is applied, the weights of the network are adjusted in accordance with the Equation 3.

$$\Delta w_{ji}(t) = -\left[\nabla^2 E(w_{ji}(t)) + \mu I\right]^{-1} \nabla E(w_{ji}(t)) \tag{3}$$

Where:

$\nabla^2 E(w_{ji}(t))$ is a Hessian matrix and $\nabla E(w_{ji}(t))$ is the gradient. The parameter μ is multiplied by the factor β when an adjust intends to increase $E(w_{ji}(t))$. When the purpose is decrease the value $E(w_{ji}(t))$ after each step, μ is divided by β. When μ is too large, the algorithm becomes a descendent gradient, with step 1/ μ. When μ is low, the algorithm is equivalent to the algorithm Gauss-Newton (Braga et al., 2007).

The conjugate gradient algorithms are usually much faster than variable learning rate backpropagation, and are sometimes faster than resilient backpropagation, although the results vary from one problem to another. The conjugate gradient algorithms require only a little more storage than the simpler algorithms. Therefore, these algorithms are good for networks with a large number of weights (Demuth et al., 2008).

4. Database and Methods

In the region of the Leão Coal Mine there is the occurrence of granitoids of Proterozoic age that constitute the basement of the Paraná Basin in that region. Those granitoids are covered by a Paleozoic sedimentary sequence which comprises the Itararé Group and the Rio Bonito, Palermo, Irati, Serra Alta, Teresina and Rio do Rasto formations (Figure 1). That succession is remarkable for its coal beds in the Rio Bonito Formation, which constitute the main Brazilian coal deposits (Gomes et al., 2003).

The database is composed of well logs and lithofacies descriptions of the cores drilled in the above-mentioned coal mine. The site is located in mid-eastern Rio Grande do Sul State (Figure 2), with a distribution in the counties of Rio Pardo, Minas do Leão, Butiá, São Jerônimo, General Câmara and Vale Verde. Despite coal mining occurs in the area since the 1940's, the National Department of Mineral Production (DNPM) and the Brazilian Geological Survey (CPRM) carried out major mineral research projects in this area between 1975 and 1983. The data come from the project named Iruí-Butiá (CPRM, 1981), with drilled in meshes from 8x8km to 1x1km (Lopes, 1990).

The logs that were used for the training, validation and classification were analyzed and selected based on the borehole and description files from the Porto Alegre's Regional Superintendence Office of the CPRM. The eight boreholes chosen for this study were LB-132-RS, LB-137-RS, LB-138-RS, LB-139-RS, LB-141-RS, LB-143-RS, LB-148-RS and LB-207-RS.

The conversion of logs from the analogue to the digital format was done by means of the original logs printed on millimeter paper. Raster images were carefully acquired in scanners and imported onto a graphic software in order to adjust the scale and perform the well log vectorization. The vectorized logs were exported as a text file (.txt) so as to relate depth values to the gamma ray values (GR), spontaneous potential (SP), resistivity (RTV) and resistance (RTC). The data set was organized in a data bank and loaded onto the Matrix Laboratory application, MatLab, afterwards for the initial stages of the neural network structuring. The data set was normalized in interval [0;1] considering the maximum and minimum values. The training dataset comprised 28% of the data, with its respective complementary set of validation of 72%, having the latter been developed with basis on information about three wells, namely LB-137-RS, LB-138-RS and LB-148-RS. The small percentage of training data is related with the small number of the electrofacies 3 available for training purposes. As training of a neural network must consider the same number of samples for each electrofacies, the training data set was limited in 28%.

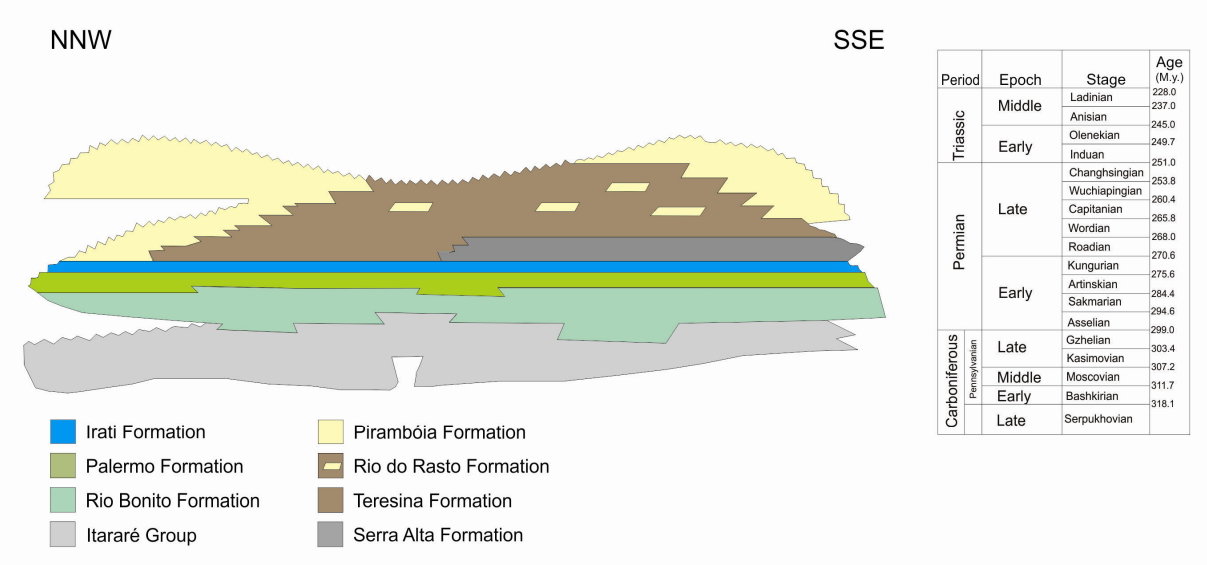

Figure 1. Stratigraphic chart of the permocarboniferous units of the Paraná Basin. Modified from Milani et al. (2007). Ages compiled from Gradstein & Ogg (2004)

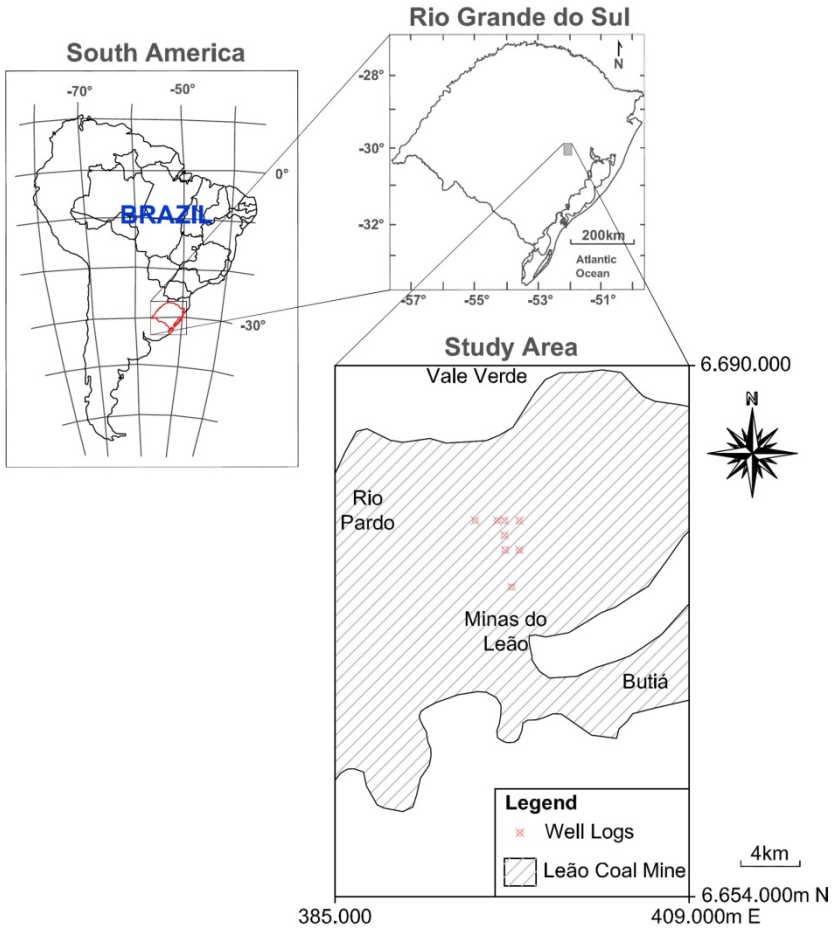

Figure 2. Location maps of the study area

In the next stage, different configuration and training algorithms were tested in order to define the appropriate neural model for the lithological classification. The lithological classes were discretized in a way that the expected output of each input came out codified. Each electrofacies pattern was related with a facies association (e.g., siltstone, sandstone and coal) and represented by a code, Electrofacies 1 = sandstone = 100, Electrofacies 2 = siltstone = 010 and Electrofacies 3 = coal = 001. The neural network was created by the Neural Network Toolbox of the MatLab application in its 7.0.1 version. A network of the multilayer perceptron (MLP) was used and its topology was defined through successive experiments (Appendix 1). The NN was developed by means of supervised learning, which means that inputs and outputs were provided with the aim of adjusting the network parameters.

To assess the performance of NN in the classification, an analysis of percentage of standards that were correctly classified, incorrectly classified, and rejected along the validation phase is done. The proportion of correctly classified standards is named accuracy. A classification is correct when the classifier matches an "unknown" standard with its true class (Braga et al., 2007). When the classifier places the "unknown" standard in the wrong class, the classification is said to be incorrect. The proportion of incorrectly classified standards gives origin to an error rate. In case the standard is similar to the standards of more than one class or is not similar enough to the standards of none of the classes, the unknown standard is then rejected, being designated as non-identified.

A simple technique that is commonly used is to present the examples to the multi-layer perceptron in a random order in between two seasons. Ideally, this random order guarantees that the examples that were successively presented to the network in one season rarely belong to the same class (Haykin, 1999).

The accuracy of the classification was checked by the Confusion Matrix (Tables 1, 2 and 3). It is a resource that offers an effective measure of the classification model by showing the number of correct classifications opposed to the classifications predicted for each class, about a group of training samples of each class. The number of

successes in each class is located in the main diagonal of the matrix. All the other elements represent errors of omission and commission in the classification (Stehman, 1997).

160 trainings were carried out until a network topology was reached and a one-percent error acceptance was set (see Appendix 1). Network input parameters were organized in the following way: one network was trained with five variables (depth, logs GR, SP, RTC, and RTV) and another one with four: depth, logs GR, SP and RTC. In all the experiments, the output had three neurons: one to represent electrofacies 1, another to represent electrofacies 2, and another one to represent electrofacies 3. The neurons work based on a non-linear function, named activation function, which determine the output data using the input data. The main activation functions are Logistic Sigmoid, Linear and Hyperbolic Tangent. The activation functions used were the linear and the logistic sigmoid function (LOGSIG), whereas the tested learning algorithms consisted of variations in the backpropagation algorithm, such as Levenberg-Marquardt, Resilient Backpropagation and Scaled Conjugate Gradient.

In the process of validation, we have tried to analyze the NN's efficiency by means of three logged and cored boreholes (LB-137-RS, LB-138-RS and LB-148-RS) with the known lithological descriptions that did not take part in the training stage. The validation set was composed of 497 samples of sandstone, 2411 of siltstone, and 263 of coal, giving a total of 3171 values. In order to assess the ability of the network classification, the complete sections of drilling that were used in the validation stage were plotted. This was done by comparing the original description with the outputs of the neural network.

5. Results and Discussions

The boreholes LB-138-RS and LB-148-RS had the best performance of learning with the topology [5-15-3-3] and as variables the logs gamma rays (GR), spontaneous potential (SP), resistivity (RTV) and resistance (RTC). The activation function used in all layers was the logistic sigmoidal, the algorithm was the Resilient backpropagation and the learning finished after 4000 cycles.

The success in the classification rate for the borehole LB-138-RS reached 76% and was the minor used in the validation stage. Electrofacies 2 reached 88,3% of success in its classification while electrofacies 1 and 3 had 51,8% and 16,5%, respectively (Table 1).

Table 1. Confusion matrix of the borehole LB-138-RS

Class	Accuracy+ (%)	Samples	Sandstone	Siltstone	Coal	NI**
Electrofacies 1 (Sandstone)	51,8	164	85	47	26	6
Electrofacies 2 (Siltstone)	88,3	797	41	704	44	8
Electrofacies 3 (Coal)	16,5	103	46	32	17	8
Total	-	1064	172	783	87	22
Accuracy* (%)	-	-	49,4	89,9	19,5	-

+ The producer's accuracy. * The user's accuracy. **Non-identified.

Although incorrectly classified as electrofacies 1 by the neural network, the interval between 219,9 a 220,5m has a number of medium-grained sandstone intercalations within a bed of siltstone. On the other hand, the interpretation of a thinner sandstone bed than that described in the core, between 222,6 and 224,3m, has to do with both silt and mud contents present as matrix of the sandstone, i.e., filling the porous space among the sand grains. The silt class tends to be enriched in potassium feldspar and the clay content of the mud is also rich in such element. In both cases, textural and mineralogical properties altered the well log patterns and affected the lithological classification. Potassium, thorium and uranium are the main radioactive element present in minerals and affect considerably the gamma rays record in well logs. The presence of silt and clay into the sandstone modify the permeability and consequently the SP, RTV and RTC logs.

This borehole also contains seven coal beds, named as S2, S3, I, I2, I3s, I3i and I4, in the interval between 256,28 and 278,55m. Thin beds are unlikely to be classified correctly due to the shoulder effect, i.e., the logging tools are not capable to record the true values of each property because the rocks situated below and above a thin interval influence the logs, creating false values between the minimum and the maximum records of contrasting rocks bounded by sharp contacts. Thus, isolated thin beds of coals are not classified correctly as electrofacies 3.

Another question is related with the wide range of possibilities involving the term coal in the study area. Coal is also used as a generic term to designate organic carbon-enriched muddy rocks. In the Leão Mine coal is characterized by a great amount of inorganic material, such as clay, silt, quartz, feldspar and lithic grains etc. In fact, the organic rocks present in the area range from coal to carbonaceous siltstones. The variable content of the inorganic material contribute to modify the log values and, consequently, the classification of the neural network. The log patterns in this interval are characterized by abrupt shifts of values, especially in the GR, RTC and RTV logs.

Electrofacies 1 was not classified with high accuracy as well, in the interval between 280,0 and 311,5m. The results of the neural network show a lot of intercalations of siltstones, and also coals, which decrease the real thickness of the sandstones. In this case, the presence of both feldspar grains and siltstone intercalations increased locally the values of the GR, RTV and RTC logs of the sandstone but SP was little or not affected. Figure 3 shows the comparison between the core log made by the geologist and that obtained from the neural network classification.

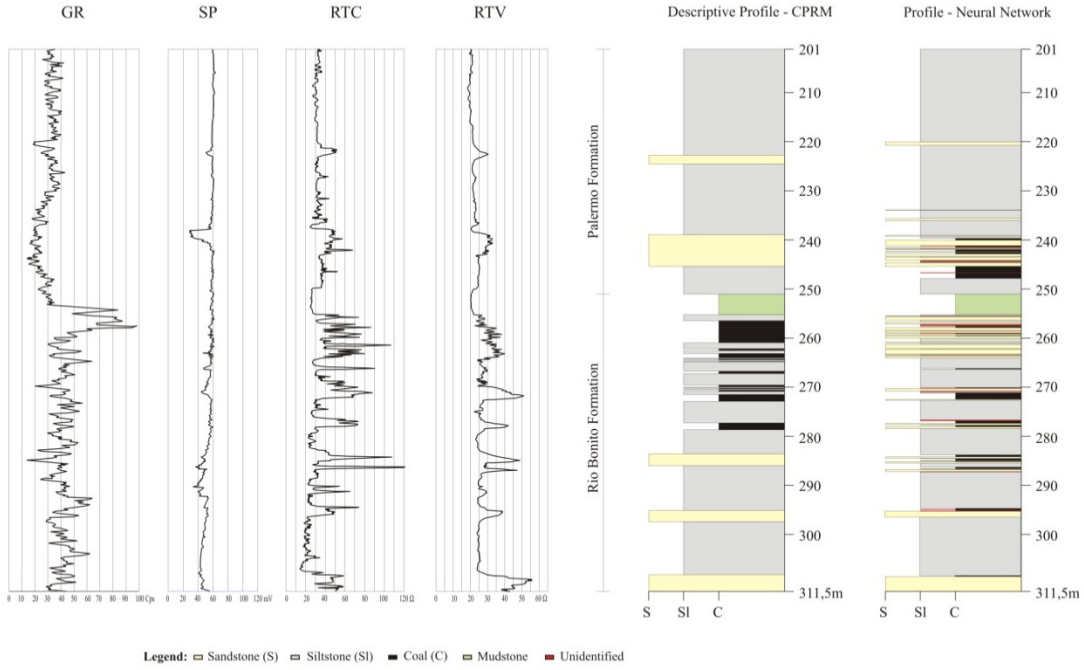

Figure 3. Comparison between the descriptive litholog of the borehole LB-138-RS of CPRM (left) and the classification performed by the neural network (right)

In the LB-148-RS the success rate was 78%, the error rate was 20% and 2% corresponds to non-identified patterns, all of them related with the validation stage. Electrofacies 2 reached 94,9% of success in its classification while electrofacies 1 had 9,8%. Electrofacies 3 was not classified in this borehole (Table 2).

Table 2. Confusion Matrix of the Borehole LB-148-RS

Class	Accuracy+ (%)	Samples	Sandstone	Siltstone	Coal	NI**
Electrofacies 1 (Sandstone)	9,8	123	12	97	8	6
Electrofacies 2 (Siltstone)	94,9	869	24	825	10	10
Electrofacies 3 (Coal)	0,0	80	4	76	0	0
Total	-	1072	40	988	18	16
Accuracy* (%)	-	-	30,0	82,7	00,0	-

+ The producer's accuracy. * The user's accuracy. ** Non-identified.

The incorrect classification between 245,4 and 245,9m resulted from the generalization for training purposes. Defined as siltstone in a minor scale, this interval contains a lot of millimetrical to centimetrical sandstone intercalations, only recognizable in a major scale of observation and description such as that of the core log. The neural network classified an intercalation of non-identified, coal and sandstone, from the base to the top, within the siltstone interval. It is quite important to calibrate the resolutions of the neural network, of the logging tools and the description performed by geologists. The resolution of the logging tools is up to 30cm therefore any thinner layer classified by the neural network must be inspected by a log analyst. This inspection can reveal, for instance, the reason for the incorrect classification of coal in the above-mentioned interval. In this case, coal resulted from a combination of specific values of the GR, RTV and RTC logs caused by the shoulder effect.

On the other hand, electrofacies 1 between 261,0 and 273, 29m was poorly classified by the neural network. The inspection of the core log has revealed that the electrofacies 1 in this interval comprises sandstone with milli-to-centimetrical intercalations of siltstones between 261,0 and 269,0m. From 269,0 to 273,29m silt is present as matrix of the sandstone in variable proportions, locally being considered as a sandy siltstone. For the depth of 318,9m, the network incorrectly classified the interval as electrofacies 1. However, in the descriptive profile, the layer of sandstone shows fine to medium grain size only in the range from 317 to 317,40m.

This borehole contains eight coal beds, named S2s, S2m, S2i, S3, I, I2, I3 and I4, between 277,93 and 297,80m. The incorrect classification of the coal beds, i.e. electrofacies 3, can be explained by their composition; in fact, they are very carbonaceous black siltstones. The comparison between the core log and that obtained from the neural network classification is shown in the Figure 4.

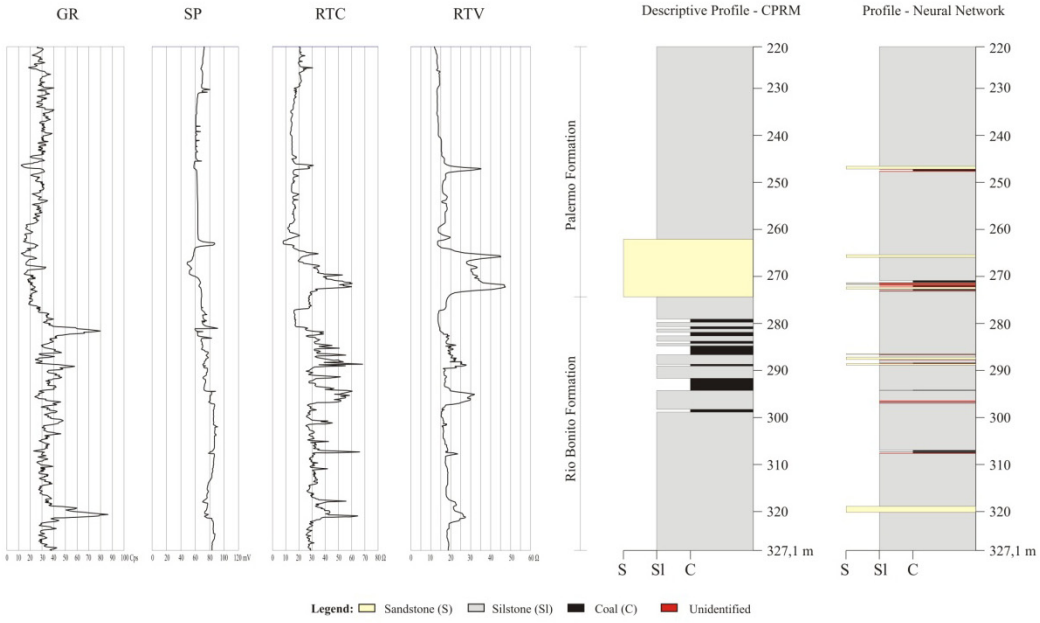

Figure 4. Comparison between the descriptive litholog of the borehole LB-148-RS of CPRM (left) and the classification done by the neural network (right)

The boreholes LB-137-RS was adjusted with a multi-layer model and had the best performance of learning with the topology [5-15-3-3], using as variables depth and the logs gamma rays (GR), spontaneous potential (SP) and resistance (RTC). The activation function used in all layers was the logistic sigmoidal, the algorithm was the Levenberg-Marquardt and the learning finished after 2000 cycles.

The success in the classification rate for this borehole during the validation stage reached 81% while errors and non-identified patterns reached 18% and 1%, respectively. Electrofacies 2 reached 93,6% of success rate and electrofacies 3 was correctly classified in 57,5% of the samples. Electrofacies 1 had the minor success rate with 43,3% (Table 3).

Table 3. Confusion Matrix of the Borehole LB-137-RS

Class	Accuracy+ (%)	Samples	Sandstone	Siltstone	Coal	NI**
Electrofacies 1 (Sandstone)	43,3	210	91	97	16	6
Electrofacies 2 (Siltstone)	93,6	745	9	697	33	6
Electrofacies 3 (Coal)	57,5	80	0	32	46	2
Total	-	1035	100	826	95	14
Accuracy* (%)	-	-	91,0	84,4	48,4	-

+ The producer's accuracy. * The user's accuracy. ** Non-identified.

The main reason for the incorrect classification of the electrofacies 1 situated between 223,60 and 225,40m is the presence of many intercalation of siltstones, which increase the GR and RTC values and decrease the SP one, and the small number of samples of these thin sandstone bed. As in the LB-148-RS, scale of description *versus* scale of sampling for training of the neural network was involved in problems for recognizing sandstones.

Several intercalations generated by the neural network classification in the interval between 240,73 and 253,86m have to do with the wide range of values of the GR, SP and RTC logs. This interval was defined as electrofacies 1 in the scale of observation and description and used as electrofacies 1 for training purposes. However, the neural network provided a different result. Electrofacies 2 and 3 were classified as centi-to-decimetric intercalations (Figure 5). The wide range of values of the well logs results of a combination of the lithological characteristics. The presence of calcite as a cement alters the pattern of the RTC and SP logs while siltstone intercalations and feldspar grains increase the GR log, promoting the classification as electrofacies 2 and 3.

The seven layers of electrofacies 3 described in the cores, named as S2s, S2I, S3, I, I2, I3 and I4 occur as intercalations among siltstone beds in the middle of the borehole LB-137-RS, between 253,90 and 277,31m (Figure 5). The electrofacies 3 classified by the neural network do not correspond with the depths of the core. However, intercalations between electrofacies 3 and 2 are the result provided by the neural network as those present in the middle portion of the core, together with some non-identified intervals. A reason for this difference in the depths is the cumulative error associated with both drilling operations and core measurements.

The drilling operation that recovers cores is performed by introducing drill bits sequentially into the borehole. The measurement of the cored interval is made based on the number of drill bits introduced in that interval. Thus, the more bits are used the more will be the error in the end of the operation. After removed from the drill bit, cores usually become bigger in length, either by the expansion promoted by the difference of pressure or by the number of fractures generated by the core drill operation. Hydration of mud-rocks containing smectites can also promote expansion of the cores. Therefore, is normal that cores have about 5 to 10% more in length than originally recovered from the borehole. Many times the core description is performed without considering this difference, expanding the real thickness of the rocks, especially muddy siltstones and claystones. On the other hand, the log tools perform measurements *in situ*, in which they are introduced at the bottom of the borehole and pulled up using cables. This type of measurements is also inclined toward problems, once that in small diameter boreholes as LB-137, LB-138 and LB-148, the logging is performed separately, i.e., GR, SP and RTC/RTV logs are acquired in different operations. This results in non-adjusted depths among the geophysical logs when different log acquisitions are not correctly calibrated. The borehole LB-137 exhibit at least three good examples of how this above-mentioned situation impacted the classification of sandstones by the neural network. The base of the electrofacies 1 in the GR log at approximately 295,0m is not coincident with both SP and RTC logs and the core log. Consequently, just a thin bed of electrofacies 1 was classified in the neural network log although sandstone in this interval is considerably thicker (see Figure5 - between 290,5 and 296,0m).

In the second case, between 241,0 and 253,0m, the RTC log is relatively about 80cm dislocated upward when horizontally compared with the SP log both at the top of this interval (see Figure 5). It was not possible to compare the GR log with SP and RTC in the same interval because the presence of potassium-bearing feldspars and clay minerals increases considerably the values of the natural radioactivity. However, their presences were not informed in the core log description and the positioning of the base of the sandstone based on the GR log would not be reliable. As a consequence, the total thickness of electrofacies 1 as described in the core log was classified by the neural network as intercalations of electrofacies 1, 2, 3 and also non-identified pattern. The description of this interval in the core log does not mention the presence of coal and mention silt only as a subordinate fraction of the sandstone.

The third example shows the GR log dislocated about 2,0 meters upward when compared with SP and RTC logs. The quartzose composition as well as the presence of carbonatic cement indicates that the electrofacies 1 is defined by a low value in the GR log, a relatively lower value in the SP log and a high value in the RTC log. They can be identified as spikes in the above-mentioned logs. However, GR spike do not correspond with SP and RTC spikes in depth (see Figure 4, between 223,61 and 225,5m). Thus, the neural network recognized the electrofacies 1 as a thin bed of electrofacies 3 intercalated within electrofacies 2. This is easily explained because the combination of values of three geophysical logs was not sufficient to characterize the electrofacies 1 as previously defined during the training and validation phases.

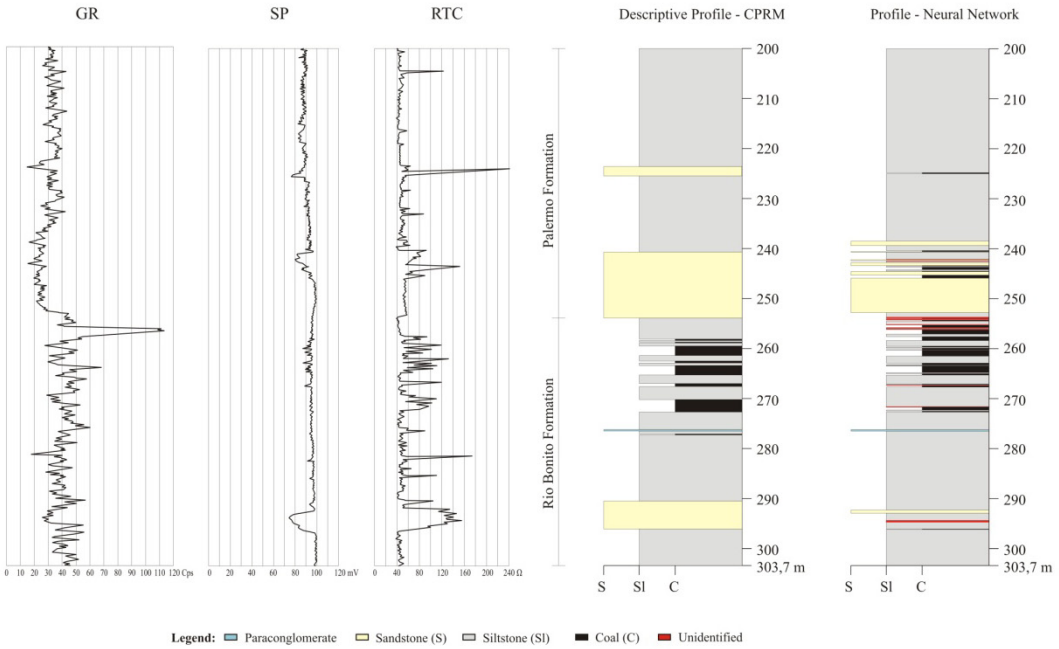

Figure 5. Comparison between the descriptive litholog of the borehole LB-137-RS of CPRM (left) and the classification done by the neural network (right)

6. Conclusions

Neural networks are a powerful and fast technique for identifying patterns and classifying rocks from well log data, especially in areas with a great number of drilled boreholes. Based on the results obtained from the study area it was possible to determine a set of important elements involving both NNs and geological aspects capable to influence the results.

The neural model used was the feedforward. Different tested parameters, such as number of hidden neurons and the number of variables as input has revealed that two intermediary layers, four variables of input and the sigmoidal logistic activation function [0;1] in all layers provided the optimal configuration. The best performance was achieved combining the above-mentioned characteristics with the Levenberg-Marquardt and Resilient backpropagation algorithms for training and validation purposes.

The accuracy of approximately 80% in the training and validation phase cannot be understood as a guarantee of high quality results. This was noted analyzing the confusion matrices of the LB-137, LB-138 and LB-148 boreholes. Electrofacies 2 had accuracy up to 88% whereas electrofacies 1 ranged from 9,8 and 51,8% and electrofacies 3 from 0 to 57,5%. A number of different factors explain the discrepancy of accuracy among the different electrofacies and their correspondent rocks, such as the difference of the scale of description with the resolution of the log acquisition, the frequent presence of silt and clay into the sandstones and coals, the abundance of potassium feldspar into the siltstones and fine-grained sandstones, the wide range of composition of the coals, the quality of the log acquisitions, the correct calibration of the geophysical logs acquired in different runs and the limited availability of appropriated logs for rock classification.

Electrofacies 2 showed the highest accuracies because they displayed the major variations of values in the logs whereas electrofacies 1 and 3 were defined by a more restricted combination of the log values. Additionally,

problems in the depth calibration of different logs contributed substantially for reducing the accuracy of sandstones and coals, especially in the boreholes LB-137 and LB-148. Despite the high complexity, this technique is a powerful resource to help geologists analyzing and classifying a massive number of boreholes bearing several logs. The fastness in obtaining interpreted data in a digital format is an additional advantage. However, the inspection of a log analyst will be always necessary to avoid problems related with both log acquisition and calibration.

Acknowledgments

The authors would like to thank the Brazilian Geological Survey (CPRM) for the availability of the well data. The Private Graduate Program (PROSUP), of CAPES, Bureau for the Qualification of Higher Education Students, is thanked for providing the Master's Degree Scholarship to PS. Contributions of the editor and of two anonymous reviewers greatly improved the manuscript.

References

Baldwin, J. L., Bateman, R. M., & Wheatley, C. L. (1990). Application of a neural network to the problem of mineral identification from well logs. *Log Analyst, 3*, 279-293.

Benaouda, D., Wadge, G., Whitmarsh, R., Rothwell, R., & McLeod, C. (1999). Inferring lithology of borehole rocks by applying neural network classifiers to downhole logs: an example from the Ocean Drilling Program. *Geophysical Journal International, 136*, 477-491.

Bhatt, A. (2002). Reservoir properties from well logs using neural networks. (Doctor thesis) – Department of Petroleum Engineering and Applied Geophysics, Norwegian University of Science and Technology, Trondheim.

Bhatt, A., & Helle, H. B. (2002). Determination of facies from well logs using modular neural networks. *Petroleum Geoscience, 8*, 217-228. http://dx.doi.org/10.1144/petgeo.8.3.217

Braga, A. P., Carvalho, A. P. L. F., & Ludermir, T. B. (2007). *Redes neurais artificiais: teorias e aplicações* (2nd ed.). Rio de Janeiro: LTC.

Busch, J. M., Fortney, W. G., & Berry, L. N. (1987). Determination of lithology from well logs by statistical analysis. *Society of Petroleum Engineers Formation Evaluation, 2*, 412-418.

CPRM – Serviço Geológico do Brasil. (1981). *Projeto Iruí-Butiá – Sísmica de Reflexão de Alta Resolução Interpretação e Avaliação – Área: Leão B. Relatório Final 1 v*. Unpublished manuscript.

Delfiner, P., Peyret, O., & Serra, O. (1987). Automatic determination of lithology from well logs. *SPE Formation Evaluation, 2*, 303-310.

Demuth, H., Beale, M., & Hagan, M. (2008). *Neural Network Toolbox™ User's Guide* (6nd ed.). MATLAB: The MathWorks™.

Derek, H., Johns, R., & Pasternack, E. (1990). Comparative study of back-propagation neural network and statistical pattern recognition techniques in identifying sandstone lithofacies. In *Proceedings 1990 Conference on Artificial Intelligence in Petroleum Exploration and Production*. College Station (pp. 41-49). Texas: Texas A & M University.

Doveton, J. H., & Cable, H. W. (1979). Fast matrix methods for the lithological interpretation of geophysical logs. In D. Gill & D. F. Merriam (Eds.), *Geomathematical and petrophysical studies in sedimentology* (pp. 101-116). Oxford: Pergamon Press, Computers in Geology Series.

Flexa, R. T., Andrade, A., & Carrasquilla, A. (2004). Identificação de litotipos nos perfis de poço do Campo de Namorado (Bacia de Campos, Brasil e do Lago Maracaibo (Venezuela) aplicando estatística multivariada. *Revista Brasileira de Geociências, 34*, 571-578.

Gomes, A. J. P., Cruz, P. R., & Borges, L. P. (2003). Recursos minerais energéticos: Carvão e Urânio. In *Geology, tectonics and mineral resources of Brazil: text maps and GIS* (p. 692). Brasília: CPRM.

Gradstein, F. M., & Ogg, J. G. (2004). Geological Time Scale 2004 – why, how, and where next. *Lethaia*, 37, 175-181.

Harris, M. H., & McCammon, R. B. (1971). A computer-oriented generalized porosity-lithology interpretation of neutron, density and sonic logs. *Journal of Petroleum Technology, 23*, 239-248. http://dx.doi.org/10.2118/2528-PA.

Haykin, S. (1999). *Neural networks: a comprehensive foundation* (2nd ed.). New Jersey: Prentice-Hall.

Hsieh, B., Lewis, C., & Lin, Z. (2005). Lithology of aquifers from geophysical well logs and fussy logic analysis: Shui-Lin Area, Taiwan. *Computers & Geosciences, 31*, 263-275. http://dx.doi.org/10.1016/j.bbr.2011.03.031

Huang, Z., & Williamson, M. A. (1996). Artificial neural network modeling as an aid to source rock characterization. *Marine and Petroleum Geology, 13*, 277-290. http://dx.doi.org/10.1016/0264-8172(95)00062-3

Ilkhchi, A. K., Rezaee, M., & Moallemi, S. A. (2006). A fuzzy logic approach for estimation of permeability and rock type from conventional well log data: an example from the Kangan reservoir in the Iran Offshore Gas Field. *Journal of Geophysics and Engineering, 3*, 356-369. http://dx.doi.org/10.1088/1742-2132/3/4/007

Lopes, R. C. (1990). Estudo paleoambiental da Formação Rio Bonito na Jazida do Leão–RS: uma análise inicial. *Estudos Tecnológicos: Acta Geologica Leopoldensia, São Leopoldo, 13*, 91-112.

Maiti, S., Tiwari, R. K., & Kumpel, H. J. (2007). Neural network modelling and classification of lithofacies using well log data: a case study from KTB borehole site. *Geophysical Journal International, 169*, 733-746. http://dx.doi.org/10.1111/j.1365-246X.2007.03342.x

Maiti, S., & Tiwari, R. K. (2010). Automatic discriminations among geophysical signals via the Bayesian neural networks approach. *Geophysics, 75*, E67-E78. http://dx.doi.org/10.1190/1.3298501.

Milani, E. J., Melo, J. H. G., Souza, P. A., Fernandes, L. A., & França, A. B. (2007). Bacia do Paraná. *Boletim de Geociências Petrobras, 15*, 265-287.

Raeesi, M., Moradzadeh, A., Ardejani, F. D., & Rahimi, M. (2012). Classification and identification of hydrocarbon reservoir lithofacies and their heterogeneity using seismic attributes, logs data and artificial neural networks. *Journal of Petroleum and Engineering, 82-83*, 151-165. http://dx.doi.org/10.1016/j.petrol.2012.01.012

Rogers, S. J., Fang, J. H., Karr, C. L., & Stanley, D. A. (1992). Determination of lithology from well logs using a neural network. *The American Association of Petroleum Geologists Bulletin, 76*, 731-739.

Saggaf, M. M., & Nebrija, Ed. L. (2000). Estimation of lithologies and depositional facies from wire-line logs. *AAPG Bulletin, 84*, 1633-1646. http://dx.doi.org/10.1306/8626BF1F-173B-11D7-8645000102C1865D

Saggaf, M. M., & Nebrija, Ed. L. (2003a). A fuzzy logic approach for the estimation of facies from wire-line logs. *AAPG Bulletin, 87*, 1223-1240. http://dx.doi.org/10.1306/02260301019

Saggaf, M. M., & Nebrija, Ed. L. (2003b). Estimation of missing logs by regularized neural networks. *AAPG Bulletin, 87*, 1377-1389. http://dx.doi.org/10.1306/03110301030

Sancevero, S. S., Remacre, A. Z., Vidal, A. C., & Portugal, R. S. (2008). Aplicação de técnicas de estatística multivariada na identificação da litologia de perfis geofísicos de poços. *Revista Brasileira de Geociências, 38*, 61-74.

Schmitt, P. (2009). Redes neurais artificiais aplicadas na classificação litológica das Formações Palermo e Rio Bonito na Jazida do Leão – RS, com base em perfis geofísicos. (Master's thesis) – Programa de Pós-Graduação em Geologia, Universidade do Vale do Rio dos Sinos, São Leopoldo, Brazil. p. 94.

Siripitayananon, P., Chen, H. C., & Hart, B. S. (2001). A new technique for lithofacies prediction: back-propagation neural network. In *Annual ACM Southeast Conference, 39th. Athens*. Georgia: New York: ACM.

Stehman, V. S. (1997). Selecting and interpreting measures of thematic classification accuracy. *Remote Sensing of Environment, 62*, 77-89. http://dx.doi.org/10.1016/S0034-4257(97)00083-7

Toumani, A., Schmitz, D., & Schepers, R. (1994). Automatic determination of lithology from well logs using fuzzy classification. In *56th Meeting of the European Association of Exploration Geophysicists*, Paper H041.

Wolff, M., & Pelissier-Combescure, J. (1982). Faciolog: Automatic Electrofacies Determination. In *SPWLA 23thAnnual Logging Symposium Conference Paper FF*.

Xuyan, W., & Zhanglong, Y. (1998). The realization of fuzzy expert system in recognizing log sedimentary facies of carbonatite section of eastern Sichuan, China. *Journal of Chengdu Institute of Technology, 25*, 60-66. http://dx.doi.org/1000-2383.0.1991-03-012

Yang, Y., Aplin, A. C., & Larter, S. R. (2004). Quantitative assessment of mudstone lithology using geophysical wireline logs and artificial neural networks. *Petroleum Geosciences, 10*, 141-151. http://dx.doi.org/10.1144/1354-079302-566

Zhang, Y., Salisch, H. A., & McPherson, J. G. (1999). Application of neural networks to identify lithofacies from well logs. *Exploration Geophysics, 30*, 45-49. http://dx.doi.org/10.1071/EG999045

Appendix 1. Characteristics of the tested neural network structures (The best results are in boldface)

Network	Training Function	Epochs	Goal	Network Topology	Performance
01	Trainrp	2000	0	[5 5 3]	0.161761
02	Trainrp	3000	0	[5 6 3]	0.127005
03	Trainrp	2000	0	[5 7 3]	0.143599
04	Trainrp	2000	0	[5 8 3]	0.126066
05	Trainrp	2000	0	[5 5 6 3]	0.137137
06	Trainrp	2000	1.00E-06	[5 6 6 3]	0.128023
07	Trainrp	4000	1.00E-06	[5 7 6 3]	0.093263
08	Trainrp	4000	1.00E-06	[5 5 8 3]	0.131707
09	Trainrp	2000	0	[5 9 3]	0.122293
10	Trainrp	4500	0	[5 9 3]	0.113562
11	Trainrp	2000	0	[5 9 3 3]	0.122020
12	Trainrp	2000	0	[5 9 5 3]	0.097517
13	Trainrp	4000	0	[5 9 5 3]	0.083604
14	Trainrp	3000	0	[5 9 7 3]	0.093627
15	Trainrp	2000	0	[5 10 3]	0.125502
16	Trainrp	3000	0	[5 10 8 3]	0.075555
17	Trainrp	2000	1.00E-06	[5 10 4 3]	0.105006
18	Trainrp	2000	0	[5 11 3]	0.102984
19	Trainrp	3000	0	[5 11 3 3]	0.121211
20	Trainrp	4000	0	[5 11 7 3]	0.887591
21	Trainrp	2000	0	[5 11 11 3]	0.073653
22	Trainrp	2000	0	[5 12 3]	0.110698
23	Trainrp	2000	0	[5 12 6 3]	0.113244
24	Trainrp	2000	0	[5 12 8 3]	0.686064
25	Trainrp	7500	0	[5 12 8 3]	0.053986
26	Trainrp	2000	0	[5 13 3]	0.110039
27	Trainrp	10000	0	[5 13 3]	0.094947
28	Trainrp	1800	0	[5 13 5 3]	0.0910092
29	Trainrp	1600	0	[5 13 5 3]	0.081546
30	Trainrp	1800	0	[5 13 9 3]	0.072645
31	Trainrp	2000	0	[5 14 3]	0.105466
32	Trainrp	1800	0	[5 14 7 3]	0.079592
33	Trainrp	6800	0	[5 14 7 3]	0.066327
34	Trainrp	2000	0	[5 15 3]	0.106643
35	**Trainrp**	**2000**	**0**	**[5 15 3 3]**	**0.101061**
36	Trainrp	100	0	[5 16 3]	0.159846
37	Trainrp	2000	0	[5 16 12 3]	0.061439
38	Trainrp	2000	0	[5 16 16 3]	0.065717
39	Trainrp	2000	0	[5 17 3]	0.101536
40	Trainrp	6500	0	[5 17 12 3]	0.040916

Network	Training Function	Epochs	Goal	Network Topology	Performance
41	Trainrp	2000	0	[5 3 3]	0.177421
42	Trainrp	2000	0	[5 4 3]	0.174565
43	Trainrp	4000	0	[5 3 4 3]	0.163174
44	Trainrp	4000	0	[5 4 2 3]	0.170973
45	Trainrp	1800	0	[5 5 2 3]	0.147313
46	Traingd	4000	0	[5 5 3]	0.212059
47	Trainlm	1200	0	[5 5 3]	0.151875
48	Trainlm	1200	0	[5 6 3]	0.396853
49	Trainlm	1200	0	[5 7 3]	0.113255
50	Trainlm	800	0	[5 8 3]	0.146548
51	Trainlm	400	0	[5 5 6 3]	0.338177
52	Trainlm	1200	0	[5 6 6 3]	0.179799
53	Trainlm	900	1.00E-10	[5 7 6 3]	0.087738
54	Trainlm	1200	1.00E-10	[5 5 8 3]	0.077445
55	Trainlm	800	0	[5 9 3]	0.097632
56	Trainlm	800	0	[5 9 3 3]	0.173424
57	Trainlm	800	0	[5 10 3]	0.152903
58	Trainlm	1200	1.00E-10	[5 10 4 3]	0.235506
59	Trainscg	1000	0	[5 10 3 3]	0.075231
60	**Trainrp**	**4000**	**0**	**[5 15 3 3]**	**0.073317**
61	Traingd	2000	0.01	[4 3 3]	0.372167
62	Trainlm	2000	0.01	[4 3 3]	0.217464
63	Trainscg	2000	0.01	[4 3 3]	0.162386
64	Trainscg	10000	0.01	[4 3 3]	0.162078
65	Traingd	2000	0.01	[4 4 3]	0.228008
66	Trainlm	955	0.01	[4 4 3]	0.157538
67	Traingd	2000	0	[4 4 3]	0.258511
68	Traingd	10000	0	[4 4 3]	0.253145
69	Traingd	2000	0	[4 4 4 3]	0.206377
70	Traingd	10000	0	[4 4 4 3]	0.168605
71	Trainlm	2000	0	[4 4 4 3]	0.114823
72	Trainlm	1000	0	[4 4 4 3]	0.114741
73	Trainscg	3000	0	[4 4 4 3]	0.127212
74	Trainscg	10000	0	[4 4 4 3]	0.120246
75	Traingd	2000	0	[4 5 3]	0.210314
76	Traingd	10000	0	[4 5 3]	0.194140
77	Trainscg	2000	0	[4 5 5 3]	0.119495
78	Trainscg	10000	0	[4 5 5 3]	0.109068
79	Trainlm	2000	0	[4 5 5 3]	0.113401
80	Traingd	2000	0	[4 6 3]	0.390762
81	Trainlm	2000	0	[4 6 3]	0.107373
82	Trainlm	10000	0	[4 6 3]	0.107011
83	Trainlm	2000	0	[4 6 6 3]	0.097712
84	Trainlm	1000	0	[4 6 6 3]	0.097708
85	Trainscg	2000	0	[4 6 6 3]	0.095146
86	Trainscg	10000	0	[4 6 6 3]	0.089533
87	Trainscg	50000	0	[4 6 6 3]	0.087341

Network	Training Function	Epochs	Goal	Network Topology	Performance
88	Trainscg	2000	0	[4 7 3]	0.133247
89	Trainscg	2000	0	[4 7 7 3]	0.120674
90	Trainscg	10000	0	[4 7 7 3]	0.097372
91	Trainlm	2000	0	[4 8 3]	0.196666
92	Trainlm	2000	0	[4 8 8 3]	0.091307
93	Trainscg	2000	0	[4 8 8 3]	0.101799
94	Trainlm	2000	0	[4 8 8 3]	0.157563
95	Trainlm	2000	0	[4 9 3]	0.109490
96	Trainlm	2000	0	[4 9 9 3]	0.033892
97	Trainscg	500	0	[4 9 9 3]	0.087229
98	Trainscg	2000	0	[4 9 9 3]	0.059246
99	Trainscg	10000	0	[4 9 9 3]	0.050717
100	Trainlm	1000	0	[4 9 9 3]	0.0689713
101	Trainscg	2000	0	[4 10 3]	0.0903861
102	Trainlm	2000	0	[4 10 3 3]	0.0793820
103	Trainscg	1000	0	[4 10 3 3]	0.0872670
104	Trainscg	1000	0	[4 10 3 3]	0.1190600
105	Trainlm	2000	0	[4 10 10 3]	0.0419324
106	Trainlm	2000	0	[4 10 10 3]	0.0559653
107	Trainlm	2000	0	[4 11 3]	0.0899211
108	Trainscg	2000	0	[4 11 3 3]	0.1047880
109	Trainscg	2000	0	[4 11 11 3]	0.0519017
110	Trainlm	1000	0	[4 11 11 3]	0.3200000
111	Trainscg	2000	0	[4 15 3 3]	0.0804826
112	Trainscg	4000	0	[4 15 3 3]	0.0596600
113	Trainlm	2000	0	[4 12 3]	0.1678090
114	Trainlm	2000	0	[4 12 6 3]	0.0367683
115	Trainlm	2000	0	[4 13 3]	0.0628424
116	Trainscg	2000	0	[4 13 13 3]	0.0418241
117	Trainscg	1000	0	[4 13 13 3]	0.0288487
118	Trainlm	2000	0	[4 14 3]	0.1982060
119	Trainlm	1000	0	[4 14 14 3]	0.0122249
120	Trainscg	2000	0	[4 14 14 3]	0.0344649
121	Trainlm	1000	0	[4 15 3 3]	0.1493460
122	Trainscg	2000	0	[4 15 3 3]	0.0707770
123	Trainscg	2000	0	[4 15 15 3]	0.2327850
124	Trainlm	2000	0	[4 16 3]	0.0637224
125	Trainlm	2000	0	[4 16 5 3]	0.1478150
126	Trainlm	2000	0	[4 16 9 3]	0.0105860
127	Trainscg	2000	0	[4 16 9 3]	0.0530648
128	Trainlm	508	0	[4 12 16 3]	0.0146699
129	Trainscg	2000	0	[4 16 14 3]	0.1354810
130	Trainlm	2000	0	[4 16 16 3]	0.0122249
131	Traingd	2000	0	[4 17 3]	0.1904250
132	Traingd	2000	0	[4 17 3]	0.1827710
133	Trainlm	500	0	[4 17 8 3]	0.2304210
134	Trainlm	463	0	[4 19 3]	0.0529747

Network	Training Function	Epochs	Goal	Network Topology	Performance
135	Trainscg	2000	0	[4 19 17 3]	0.0243736
136	Trainlm	759	0	[4 20 3]	0.0480848
137	Trainscg	2000	0	[4 20 10 3]	0.0319886
138	Trainlm	500	0	[4 25 3]	0.0516164
139	Trainlm	500	0	[4 25 10 3]	0.0219058
140	Trainscg	2000	0	[4 30 3]	0.0184589
141	Trainrp	500	0.001	[4 10 10 3]	0.0939445
142	Trainrp	2000	0.001	[4 10 10 3]	0.0690895
143	Trainrp	2000	0.001	[4 6 4 3]	0.1293610
144	Trainrp	4000	0	[4 15 3 3]	0.0842303
145	Trainrp	4000	0.001	[4 16 3 3]	0.081825
146	Trainrp	2000	0.001	[4 12 16 3]	0.0633783
147	Trainrp	2000	0.001	[4 14 17 3]	0.0536302
148	Trainrp	4000	0	[4 16 4 3]	0.0862503
149	Trainrp	2000	0	[4 40 3]	0.0758472
150	Trainlm	500	0.0001	[4 35 3]	0.0369465
151	Trainscg	1000	0.0001	[4 30 3]	0.0544163
152	Trainrp	2000	0.0001	[4 16 8 3]	0.0846655
153	Trainrp	7000	0.0000001	[4 16 8 3]	0.0610484
154	Traingd	10000	0	[4 5 3]	0.1923500
155	Traingd	4000	0	[4 4 4 3]	0.2038060
156	Trainrp	4500	0.00001	[4 4 4 3]	0.153103
157	Trainrp	200	0.001	[4 3 3 3]	0.186938
158	Trainrp	4500	0.00001	[4 16 16 3]	0.332939
159	Trainrp	3250	0.0000001	[4 17 15 3]	0.0699365
160	Trainrp	1800	0.0000001	[4 17 15 3]	0.0772765

Where:

Trainrp – Resilient backpropagation,

Traingd – Gradient descent backpropagation,

Trainlm – Levenberg-Marquardt backpropagation,

Trainscg – Scale conjugate gradient backpropagation.